



Fig 1A

$$\vec{F}_{rad} = 0$$

$$T = 2 \cdot |\vec{F}| \cdot r$$

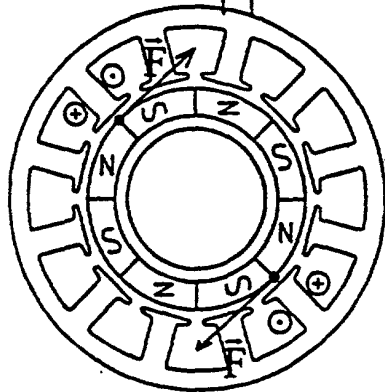
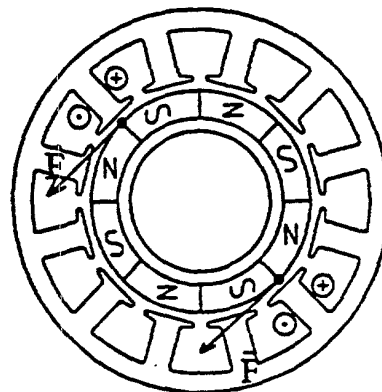


Fig 1B

$$\vec{F}_{rad} = 2 \cdot \vec{F}$$

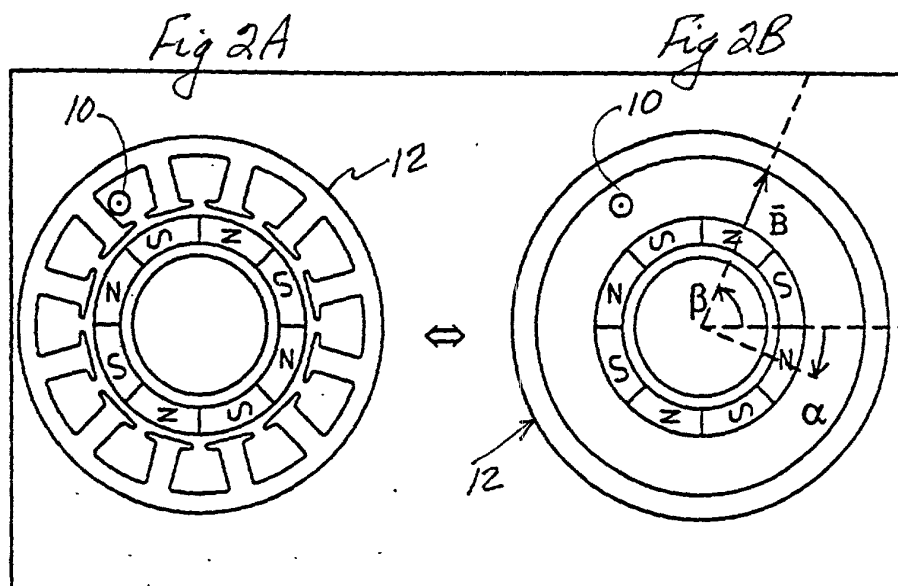
$$T = 0$$



a: 2 coils generating torque

b: 2 coils generating radial force

Fig. A.1



a: conductor placed in one slot

b: assumption that conductor is placed in the airgap

Fig. A.3

Fig. 3A

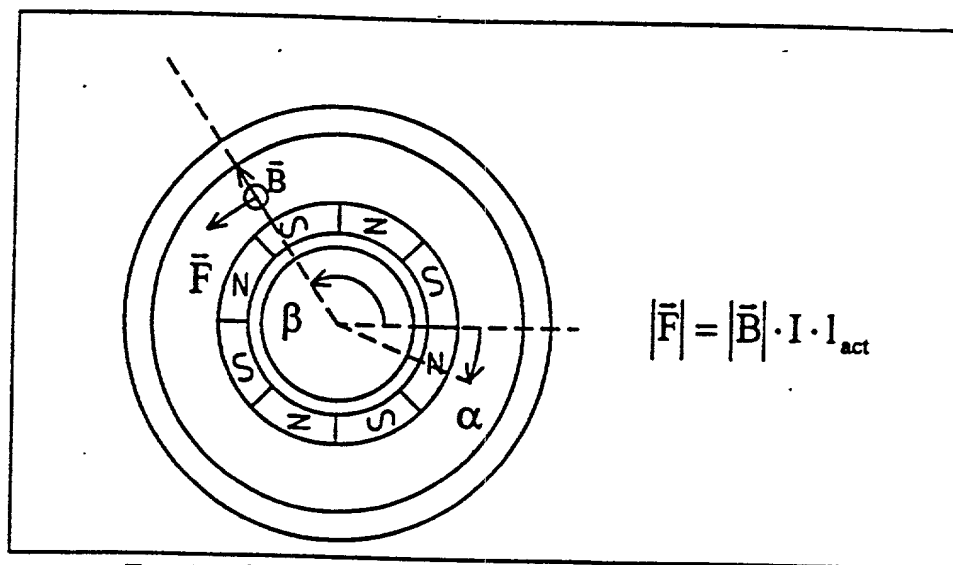


Fig. A.4: force acting on one conductor placed in the airgap

Fig. 3B

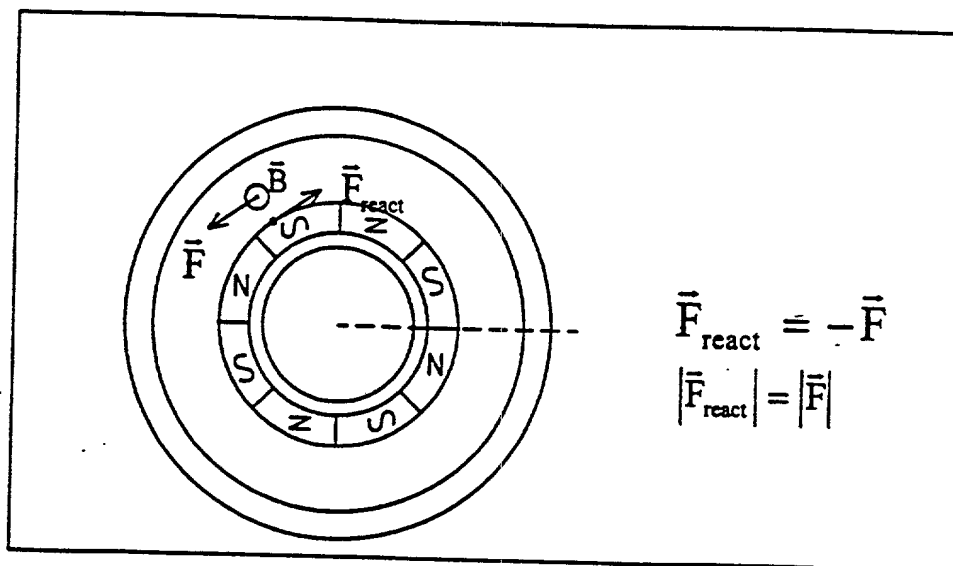


Fig. A.5: action and reaction rule, force acting on the magnet due to current flowing through the conductor placed in the airgap.

Fig. 4

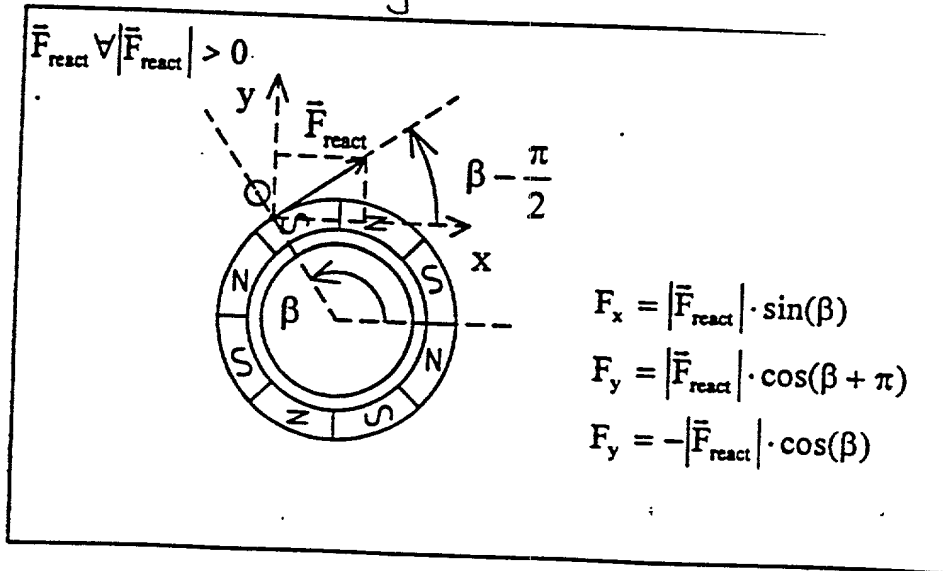


Fig. A.6: projection of the force on the x and y axis.

Fig. 5

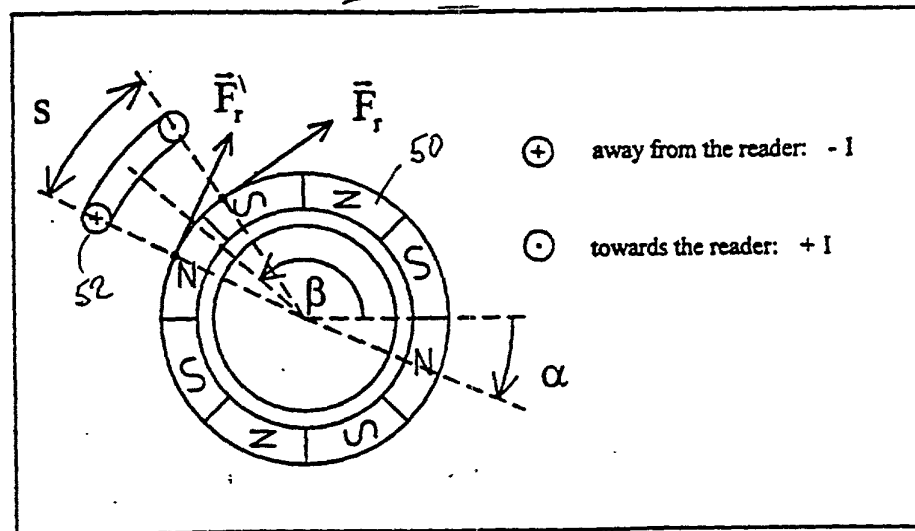


Fig. A.7: 2 forces acting on the magnet when one coil is placed in the air gap.

Fig 6A

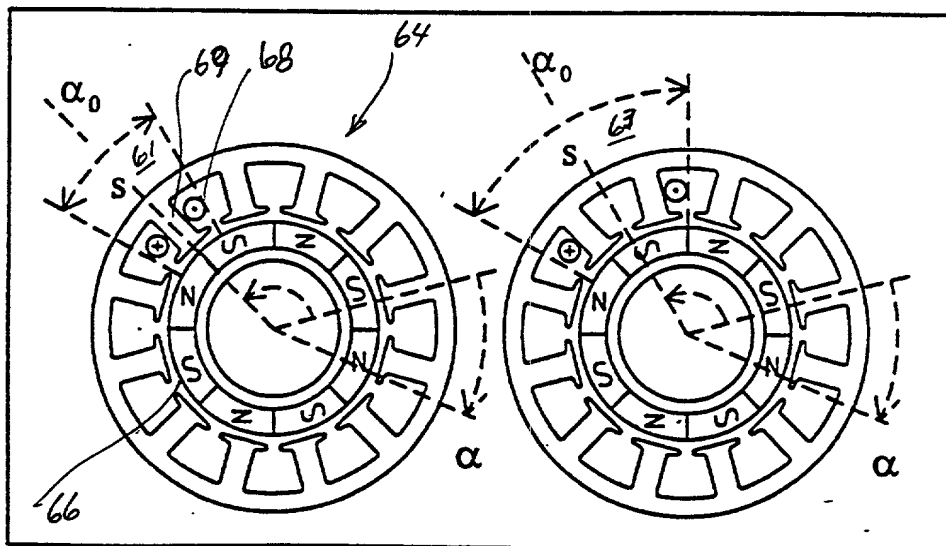


Fig 6B

a: coil opening of 1 slot

b: coil opening of 2 slots

Fig. A.8

Fig 7

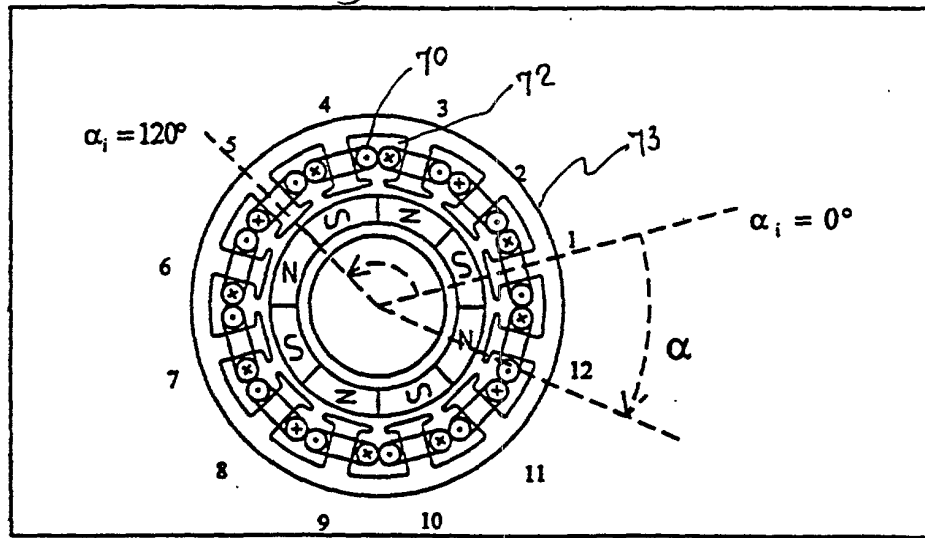
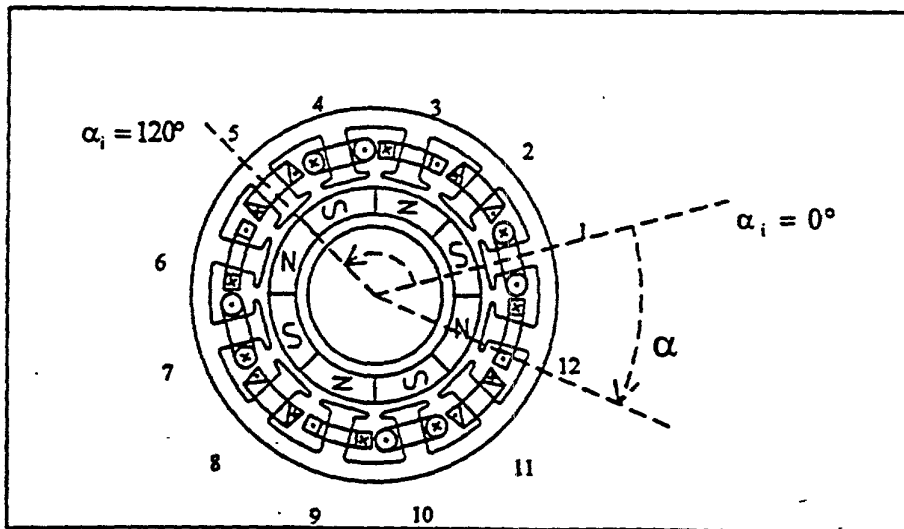
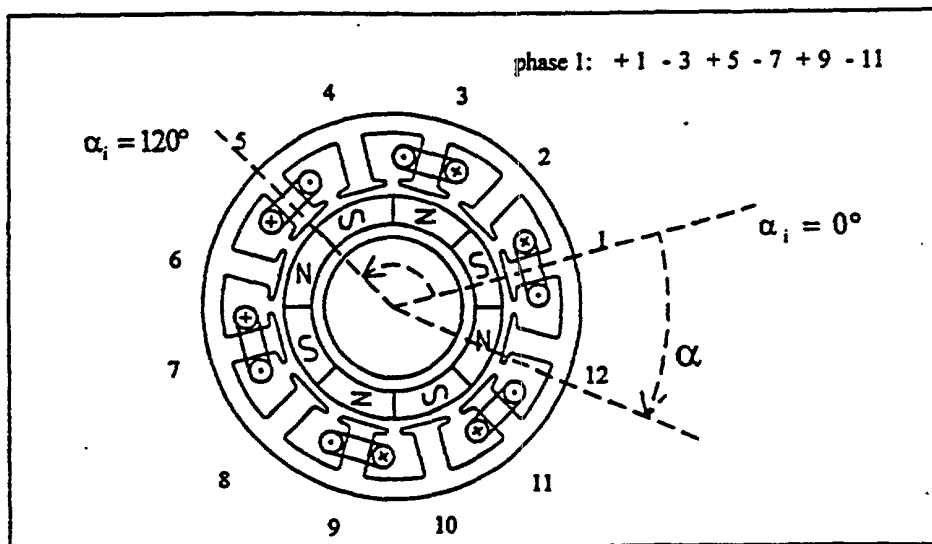


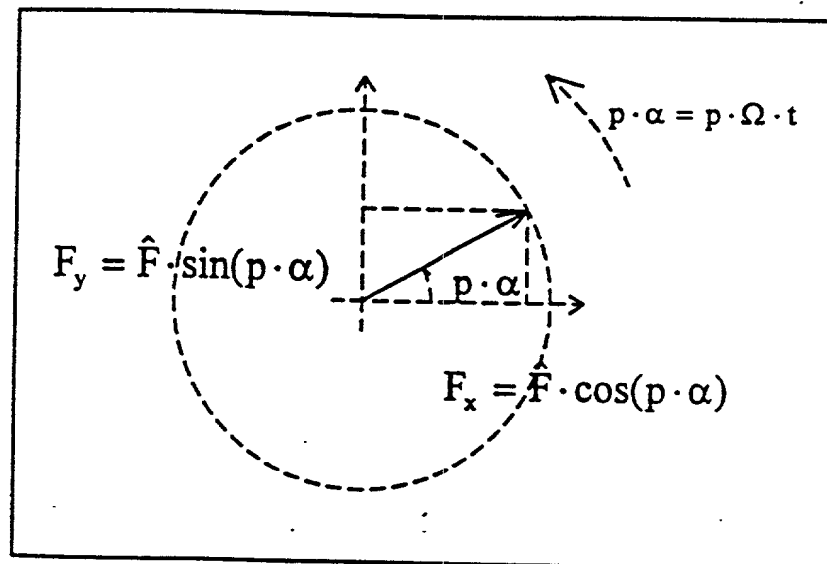
Fig. A.10: 12 concentric coils placed in the 12 slots of the motor.



8
Fig. A-12: 3 phase winding generating torque for a 8 poles 12 slots motor

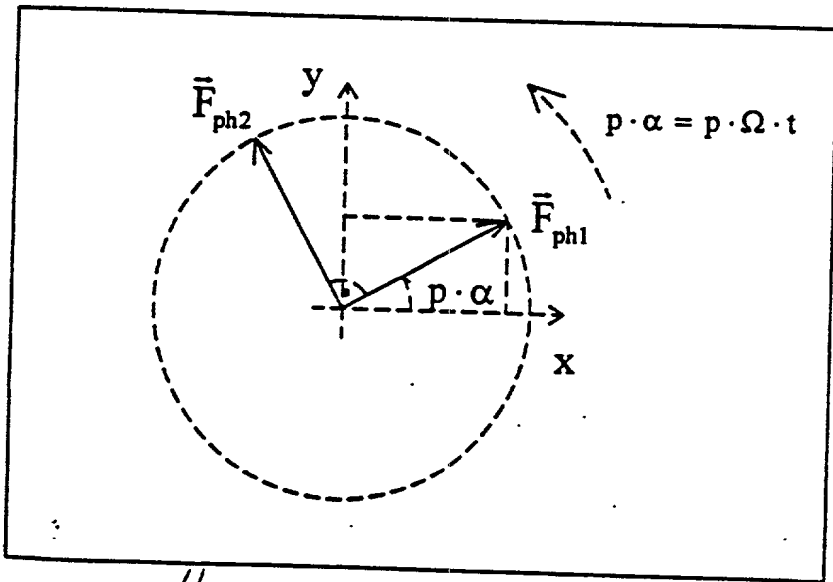


9
Fig. A.14: one phase of 6 coils generating a radial force.

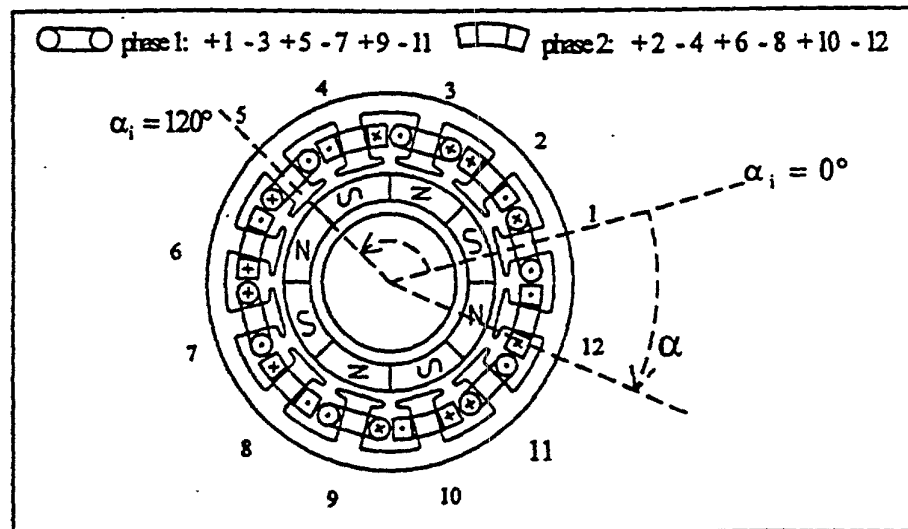


10

Fig. 4.15: one rotating radial force.

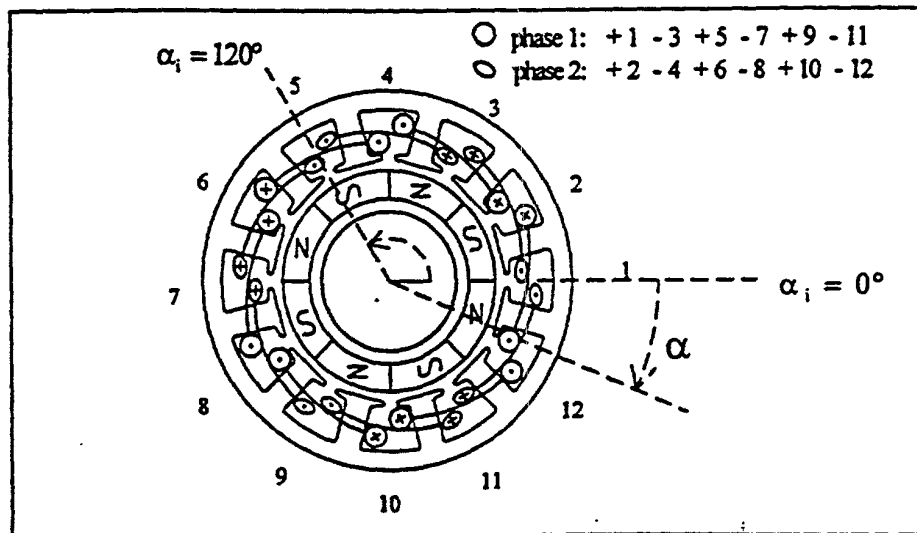


//
Fig. 4-16: 2 rotating radial forces in quadrature.



12

Fig. 4.18: 2 phase winding generating 2 radial forces in quadrature, coil-opening of 1 slot.



13

Fig. A.19: 2 phase winding generating 2 radial forces in quadrature, coil opening of 2 slots.

FIG 14A

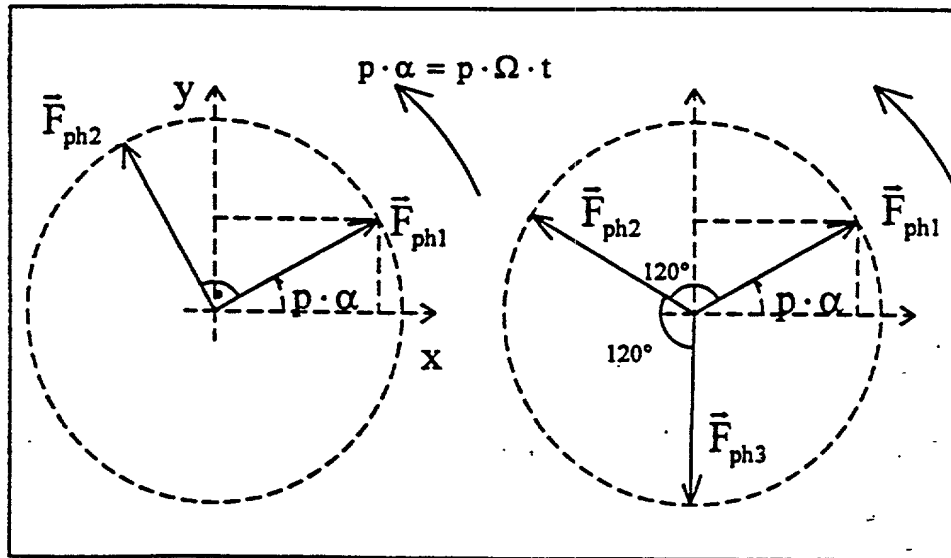
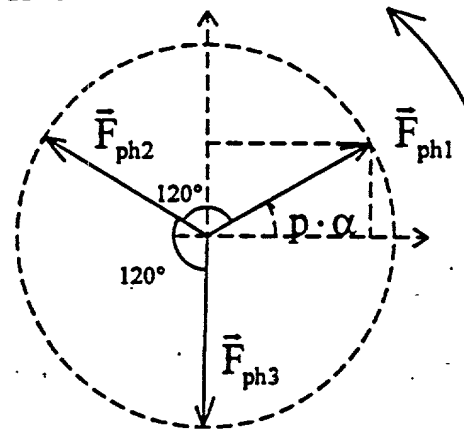


FIG 14B



a: 2 rotating forces in quadrature.

b: 3 rotating forces separated by 120° .

Fig. 425

Fig. 15

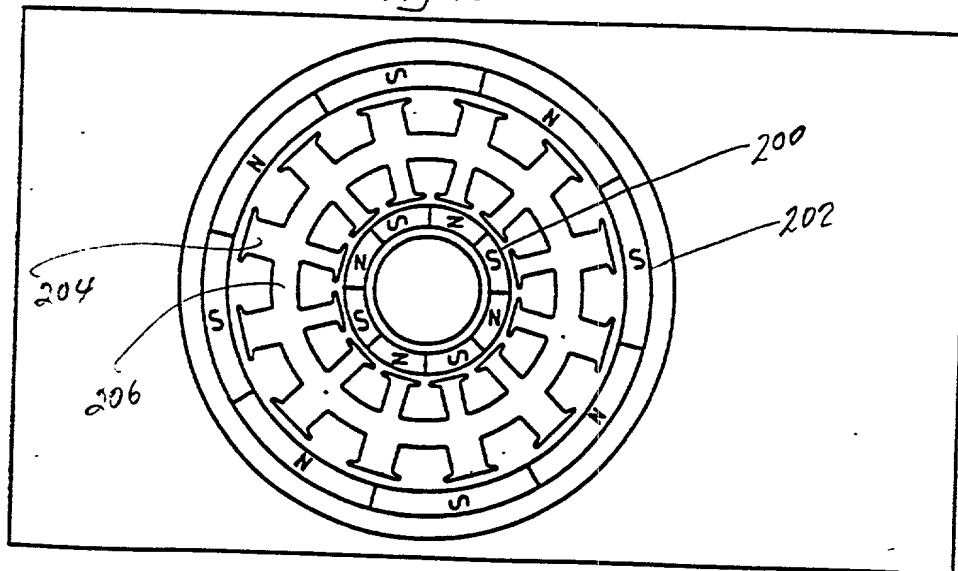
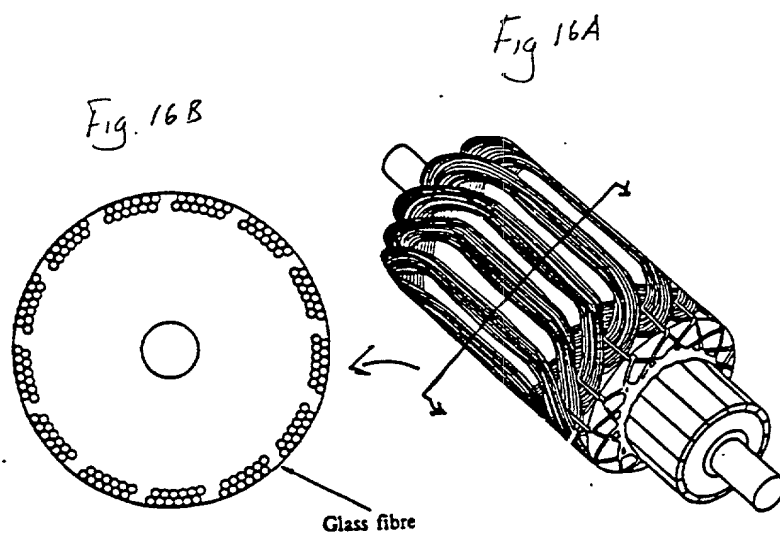


Fig. A.27: motor structure with 2 magnetic circuit.



16
 Fig. ~~A-28~~: example of a slotless motor winding (cylinder placed in the airgap).

Fig. #17

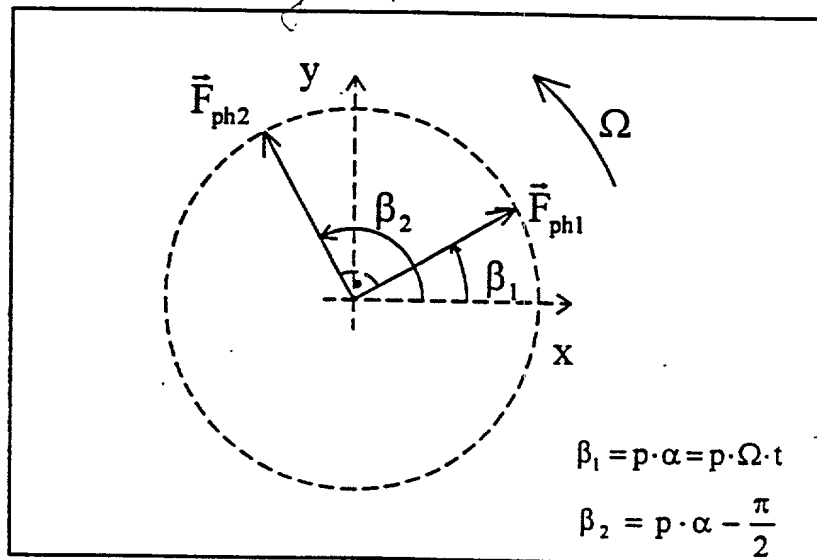


Fig. A.34: 2 rotating radial forces in quadrature.

Fig. 18

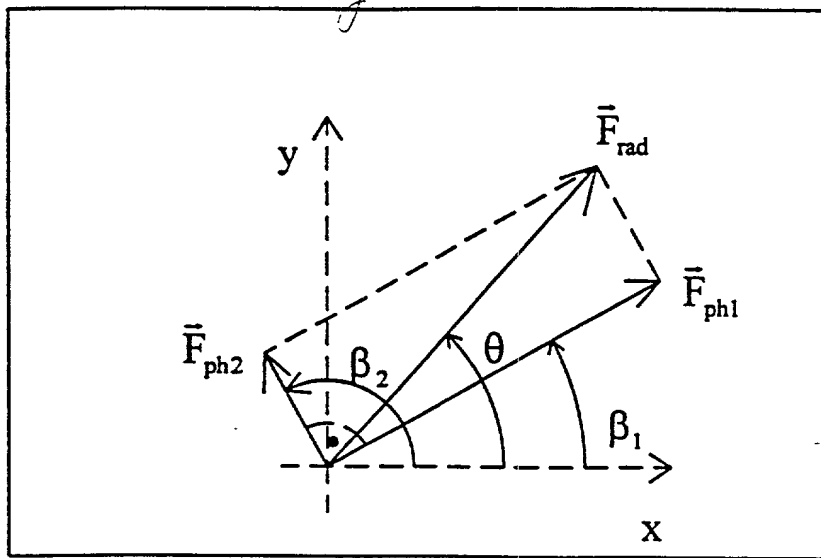
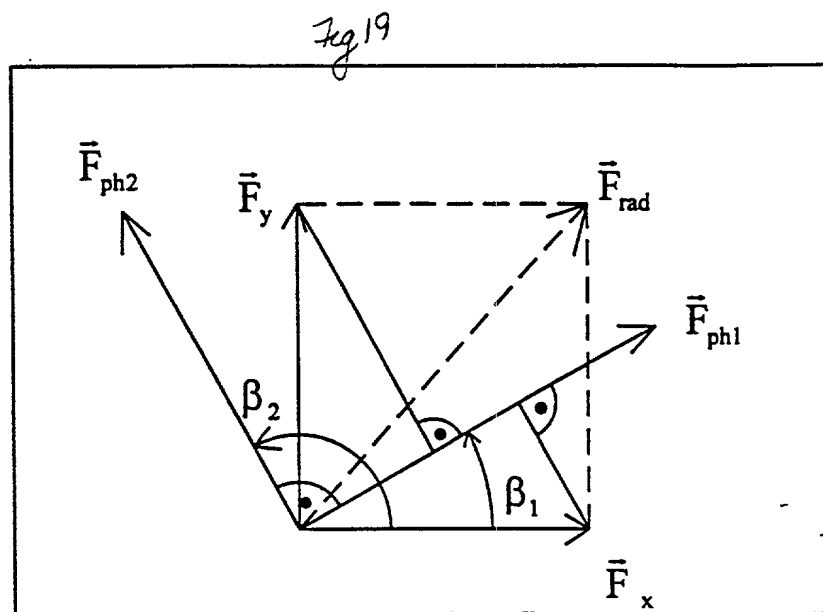
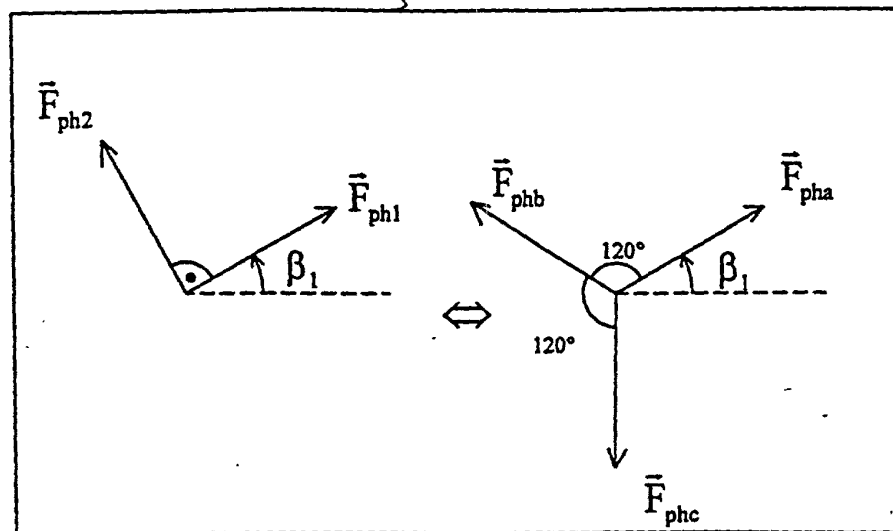


Fig. A.35: projection of the radial force vector onto the vectors of the forces generated by phases 1 and 2.



~~Fig. A.36~~ Fig. A.36: projections of the x and y radial force component vectors onto the vector of the force generated by phase 1.

Fig. 20



19

Fig. A-37: relationship between a sum of 2 forces in quadrature and a sum of 3 forces which directions are separated by 120° .

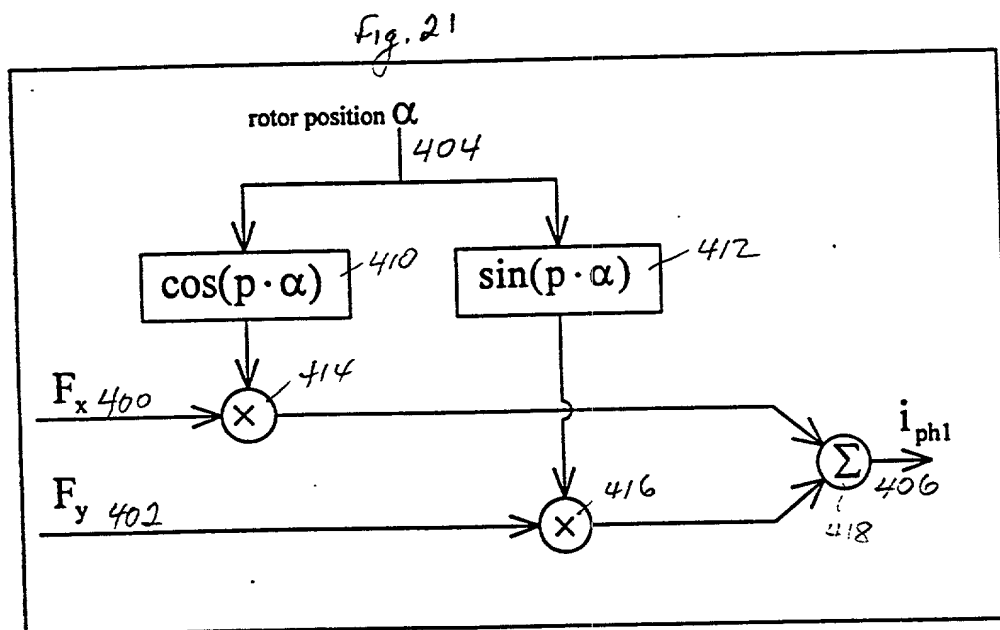
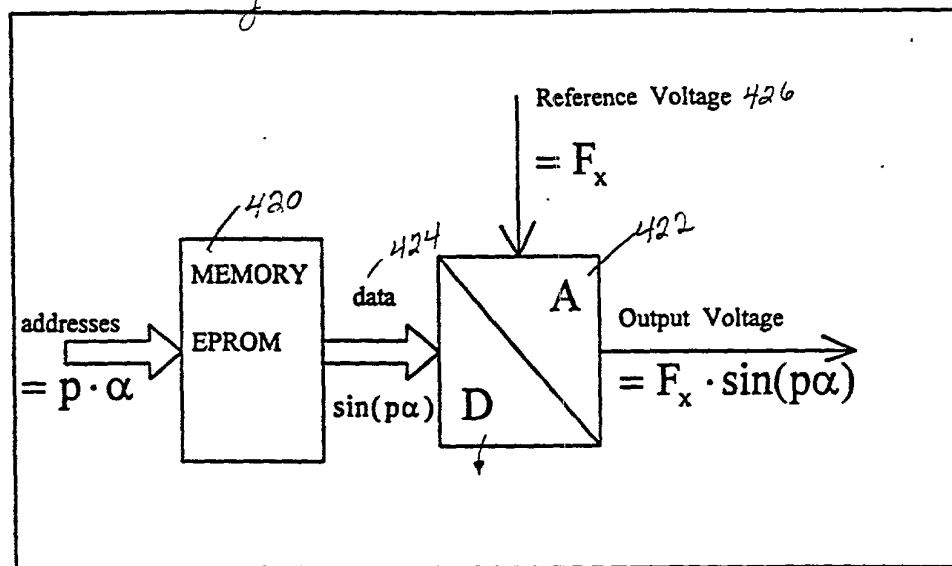


Fig. A.38: bloc diagram of the phase 1 current calculation (expression (a.59)).

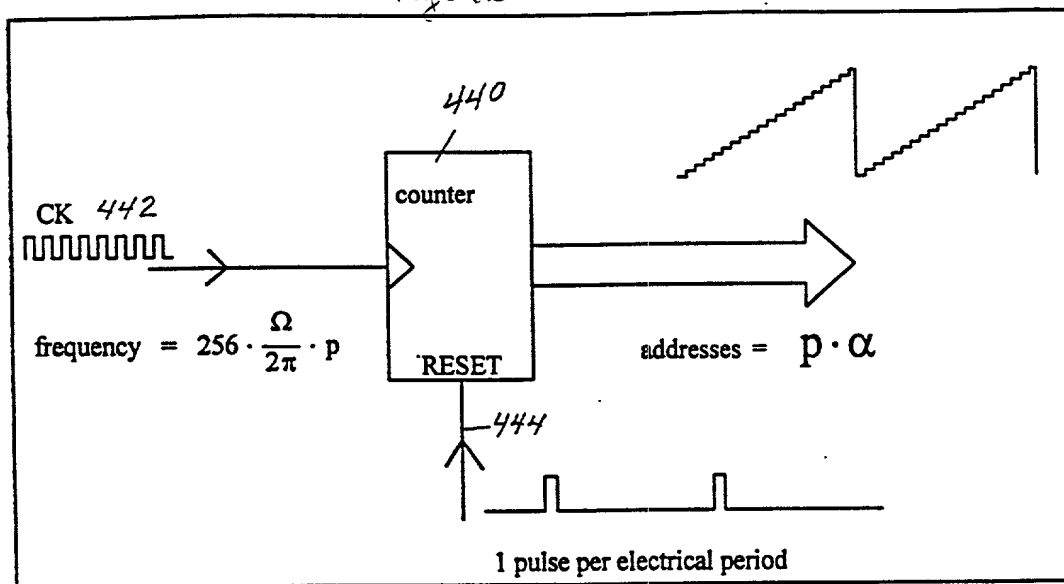
Fig 22



21

Fig. 429: electronic solution processing one trigonometric function and one multiplication.

Fig. 23



~~Fig. A-40~~ ^{for} electronic solution generating the EPROM addresses as a function of the rotor position.

Fig 24

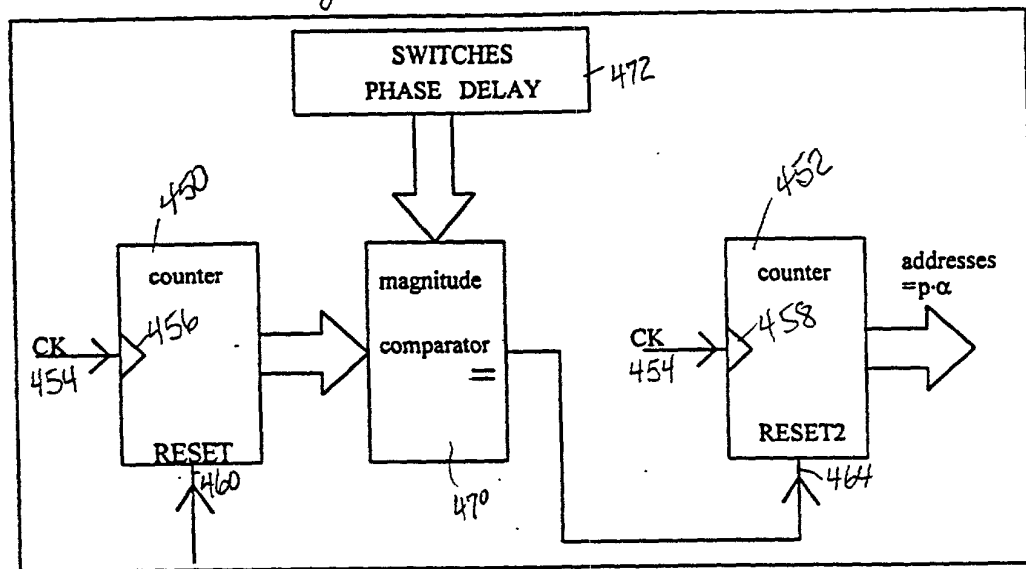


Fig. A.42: electronic solution generating the EPROM addresses as a function of the rotor position, with phase delay adjustment possibility

Fig 25

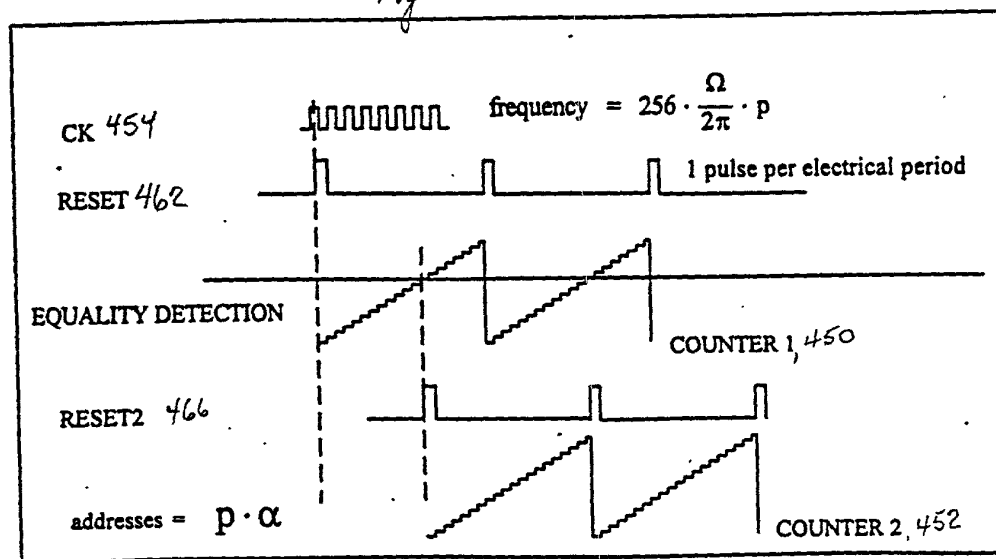


Fig A.43: Timing diagram corresponding to the electronic solution of Fig. A.42.

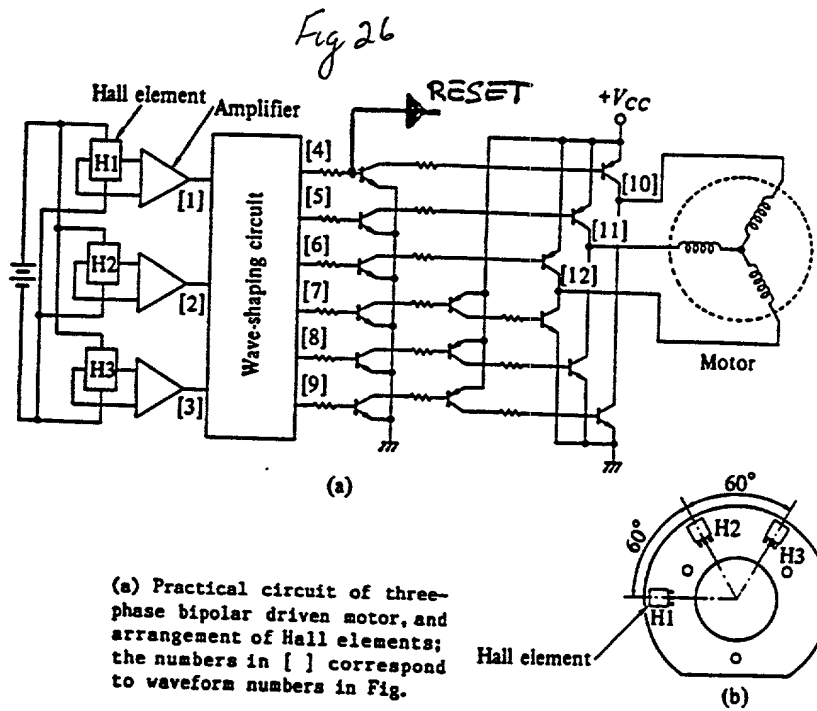
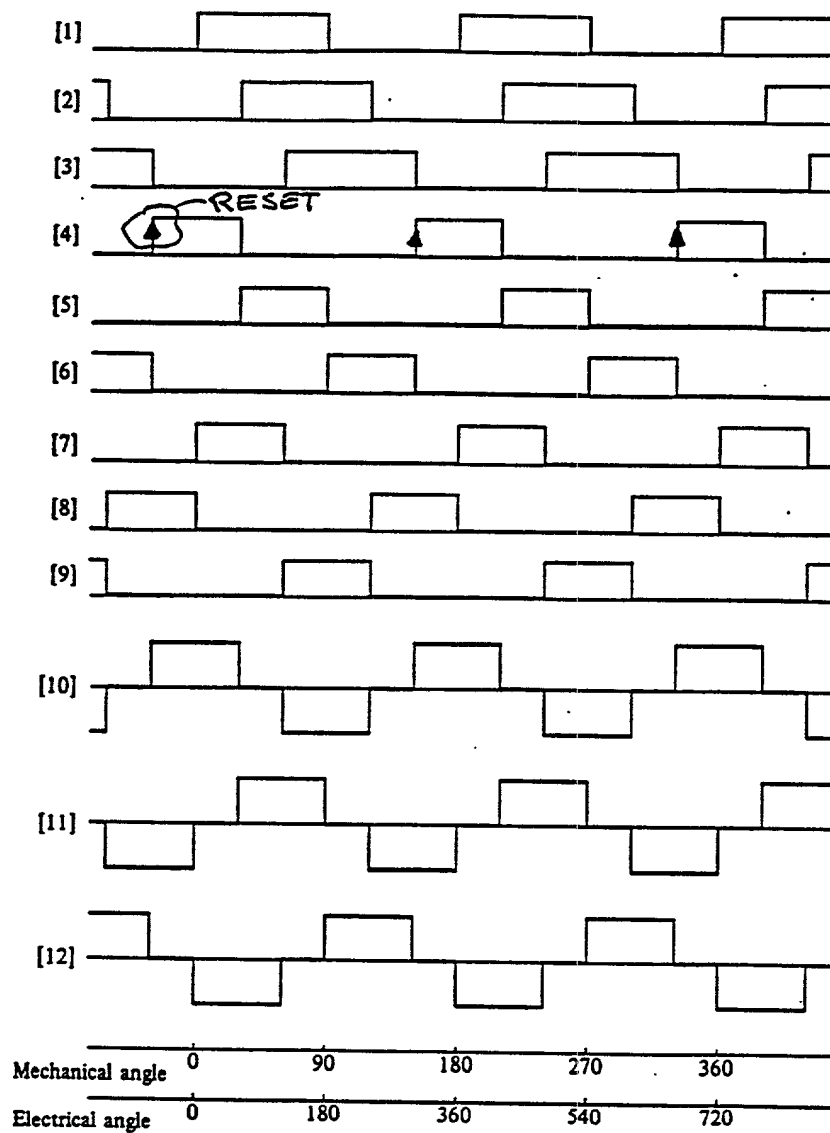


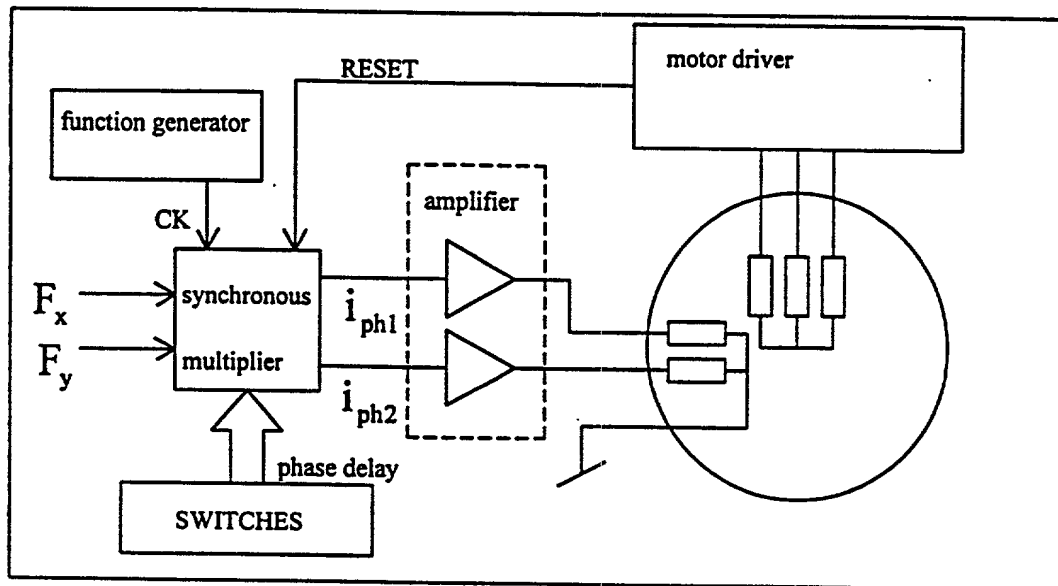
Fig. A.44: Using a transistor command signal of the motor driver to generate one pulse per electrical period.



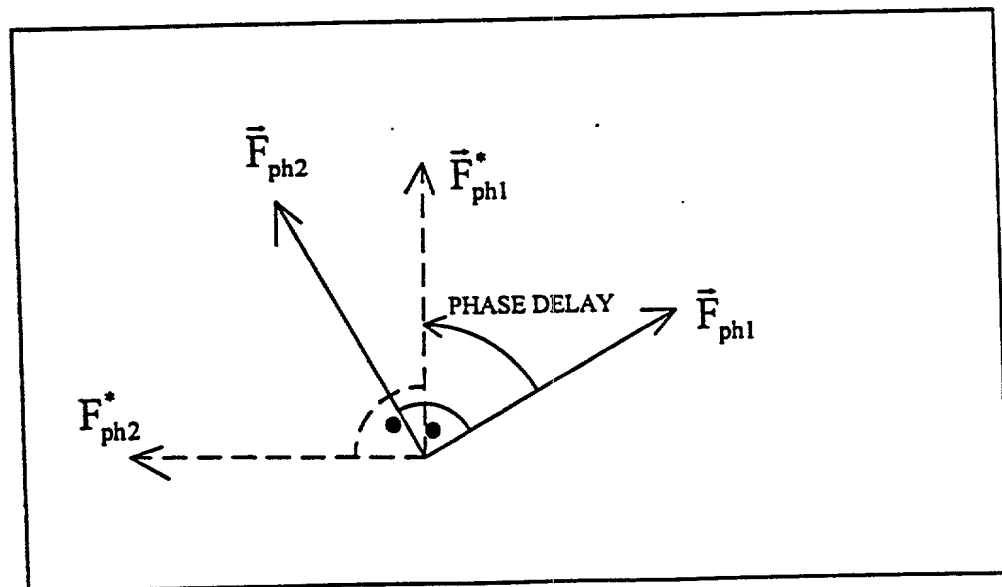
Voltage waveforms at each part (see Fig. A.44(a)).

27

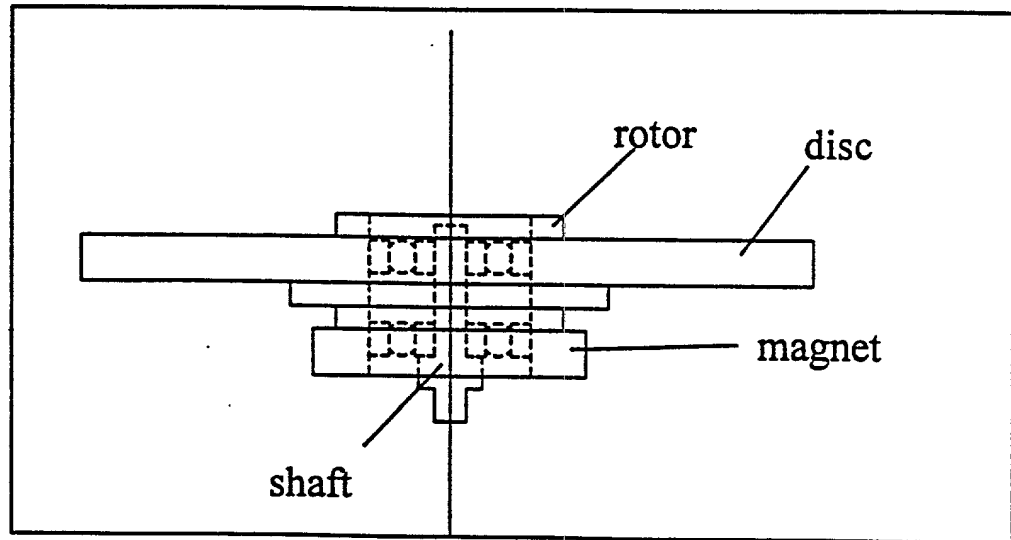
Fig. 4.45: Using a transistor command signal of the motor driver to generate one pulse per electrical period, timing diagram.



28
 Fig. A.46: final bloc diagram of the electronic supply of the 2 phase winding generating radial force.

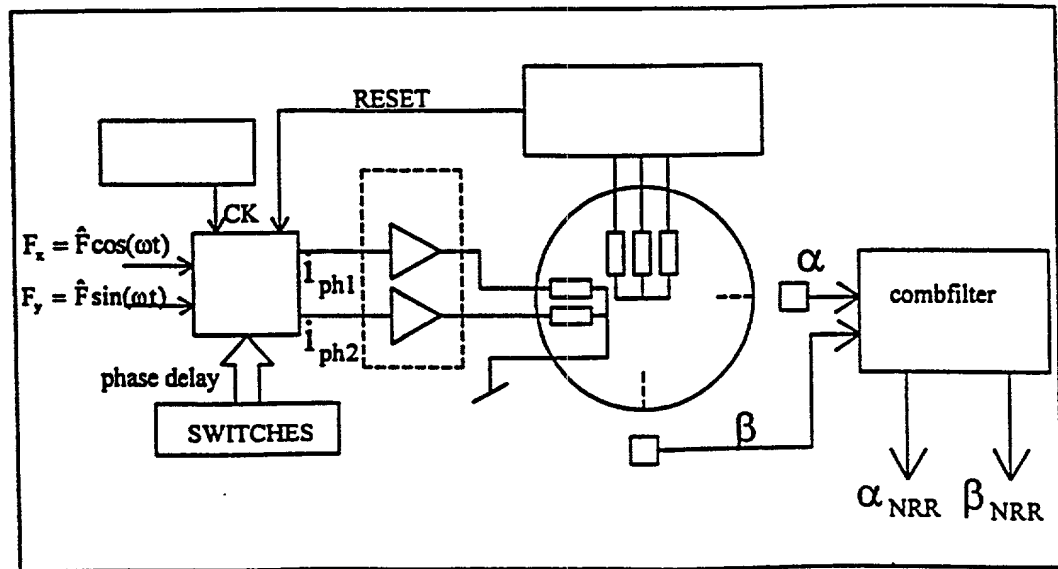


29
 Fig. A-47: phase delay effect on the radial force direction.

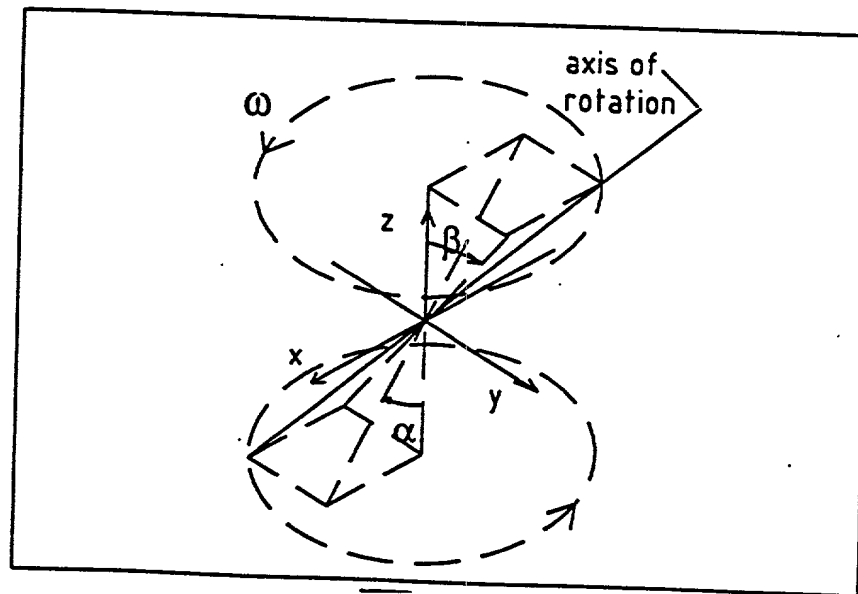


30

Fig. A-48: harddrive spindle motor.



31
Fig. A.49: measurement of the response to a rotating radial force excitation.



32
Fig. A.50: definition of the rotational axis angular position

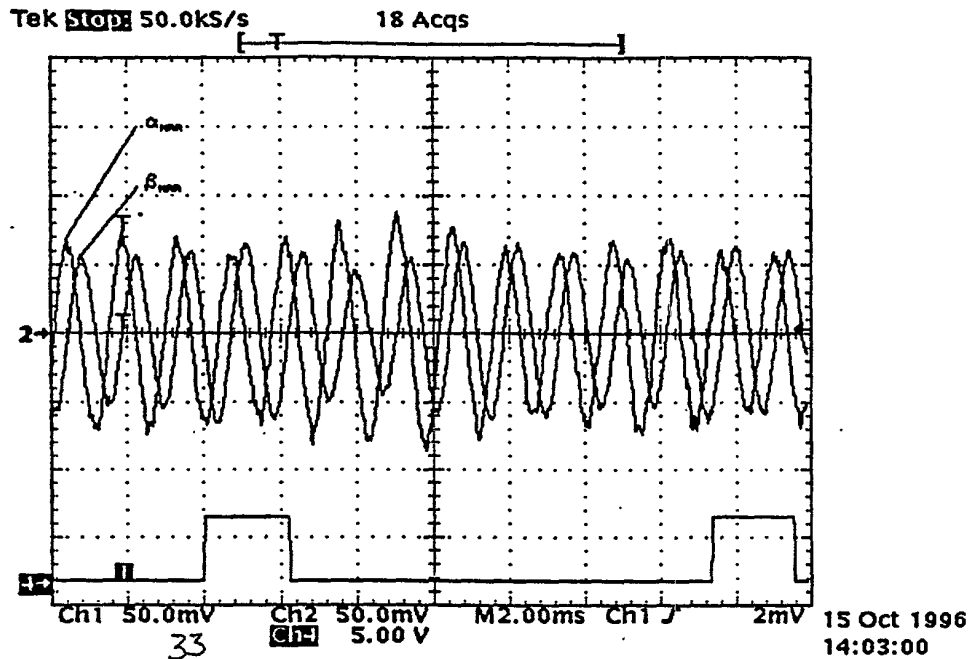
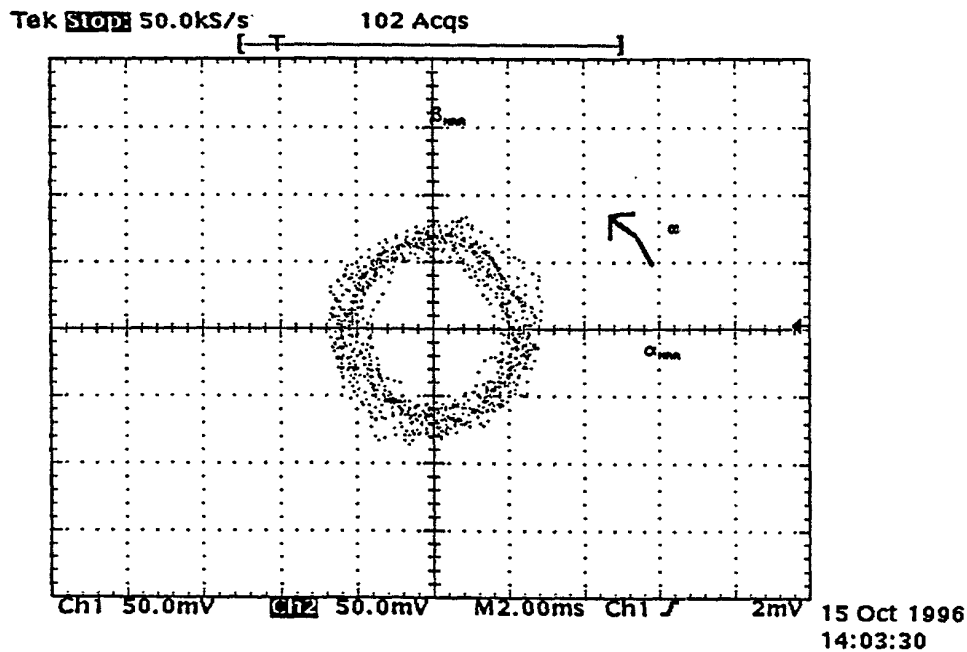


Fig. A-51: excitation of the forward gyroscopic mode, measure of the NOR components of α and β , measure of a signal giving one pulse per revolution.



34
Fig. A-52: excitation of the forward gyroscopic mode, Lissajou figure of the NRR components of α and β .

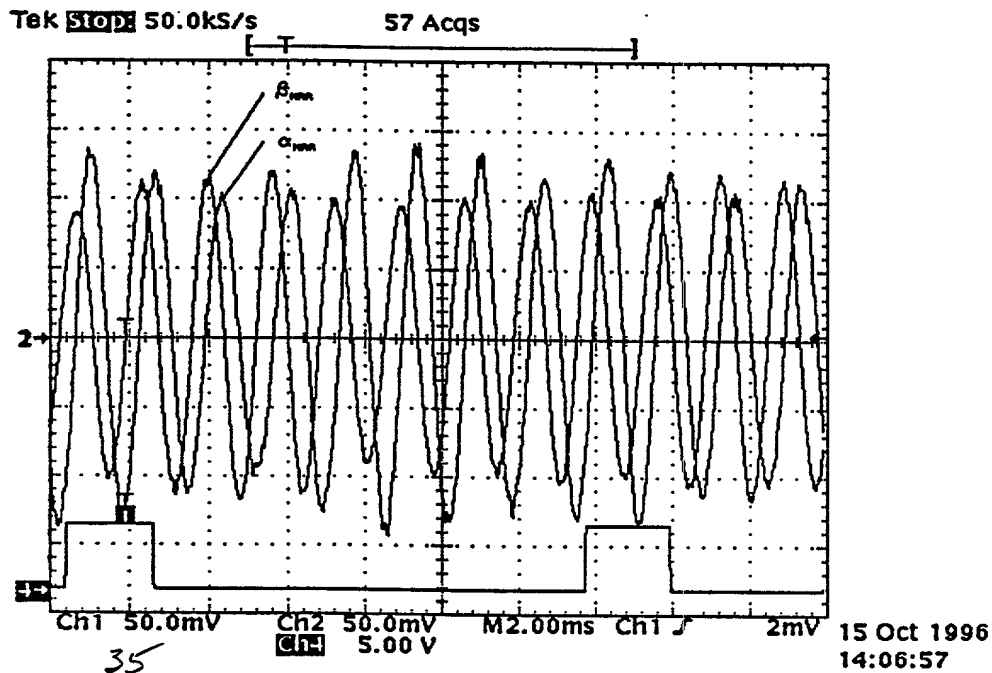


Fig. A.53: excitation of the backward gyroscopic mode, measure of the NRR components of α and β , measure of a signal giving one pulse per revolution.

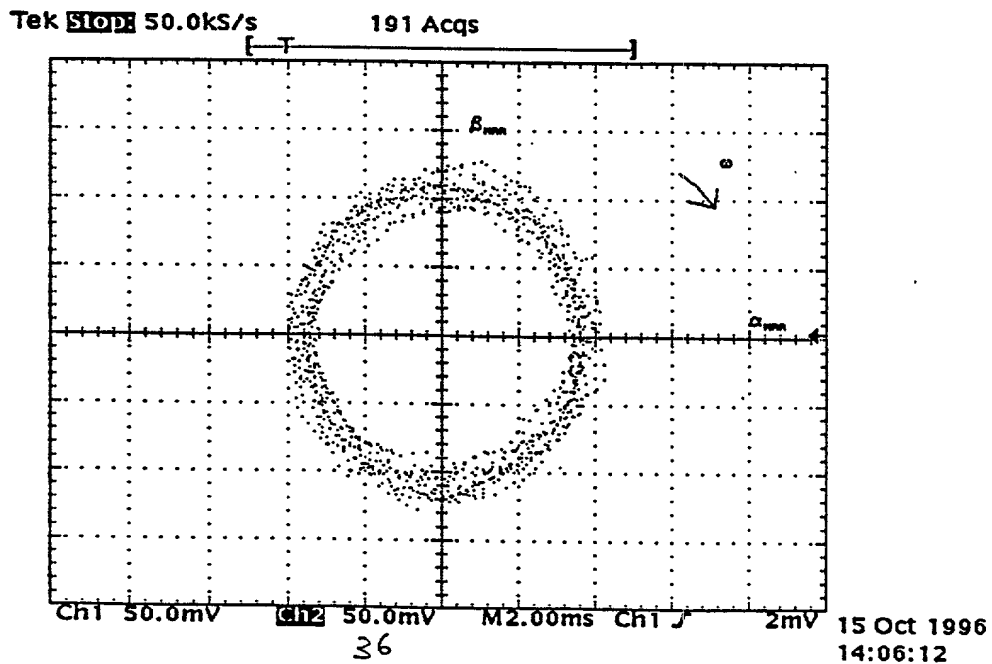
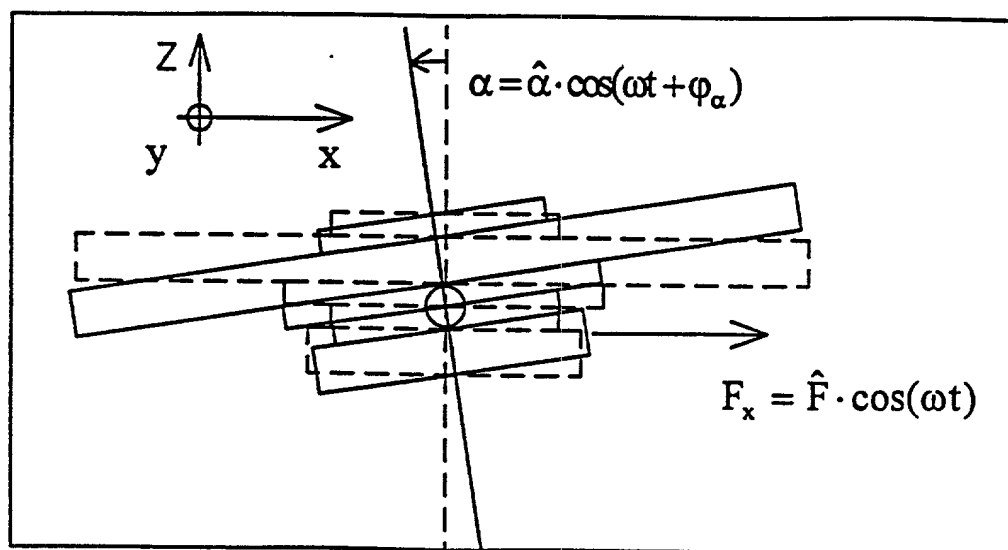
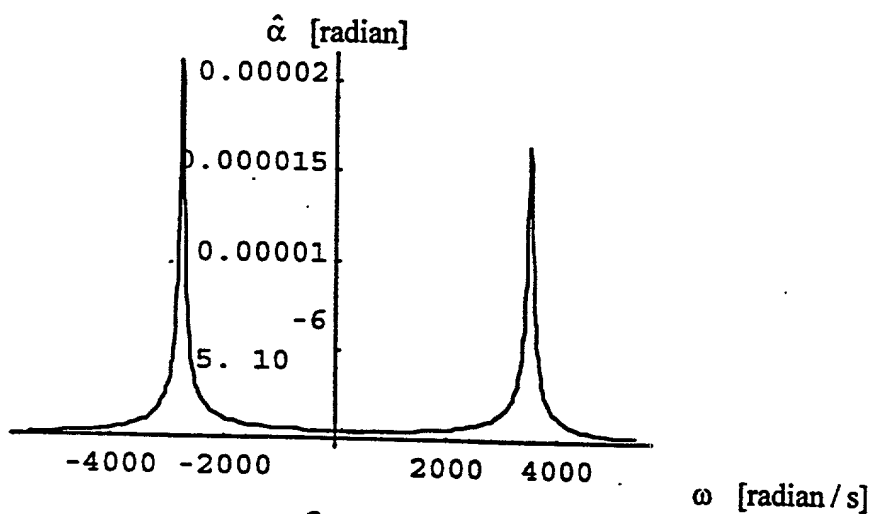


Fig. A.54: excitation of the backward gyroscopic mode, Lissajou figure of the NRR components of α and β .



37

Fig. A.55: rotor motion in plan xz .



38

Fig. A.56: Bode plot of the α wave magnitude.

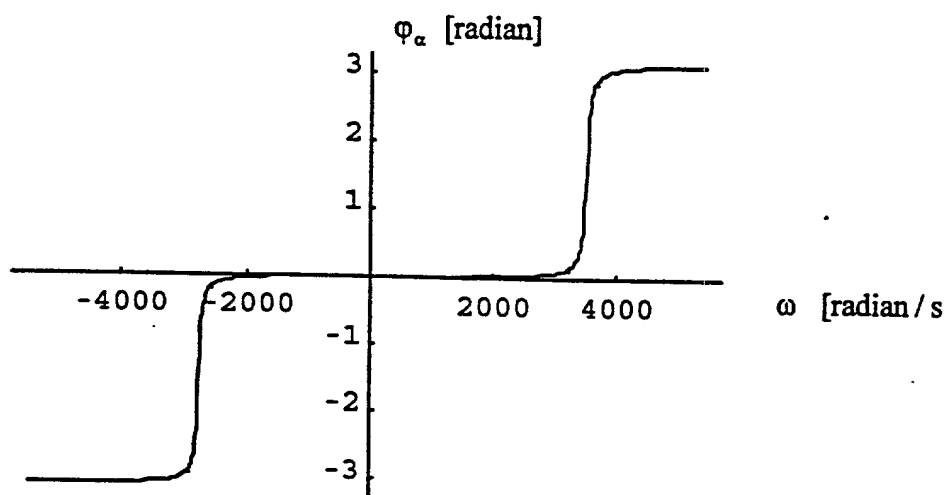


Fig. A.57: Bode plot of the α wave phase delay.

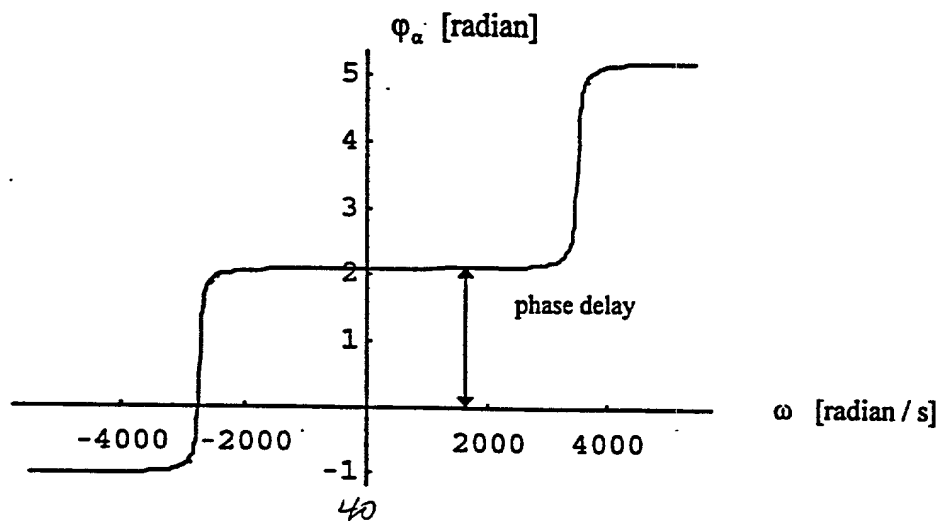


Fig. A-58: Bode plot of the α wave phase delay including the effect of the synchronous multiplier phase delay.

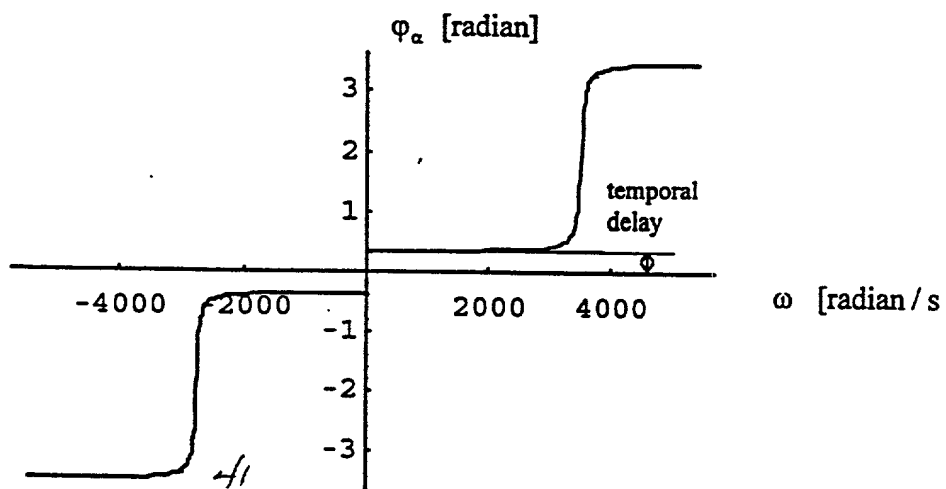
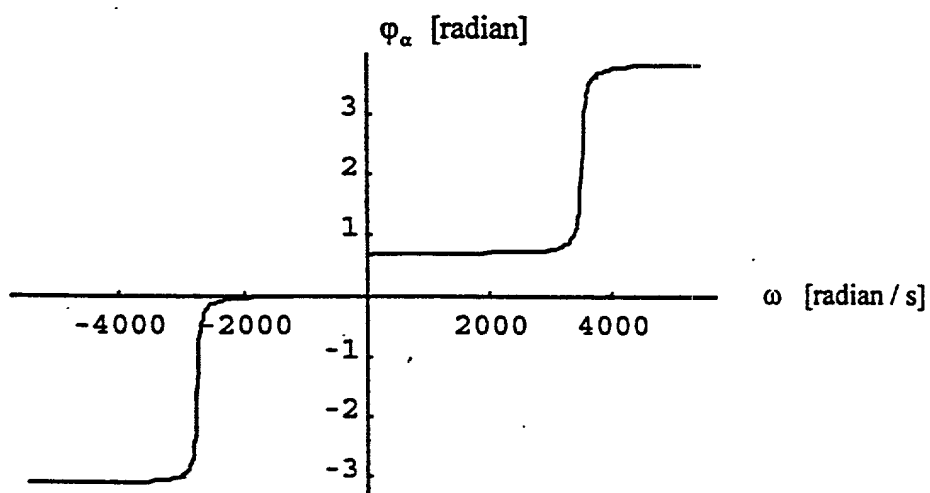


Fig. A.59: Bode plot of the α wave phase delay, including the temporal delay introduced by the current amplifiers and by the measure system.



42
 Fig. A.60: correction of the temporal delay of the backward gyroscopic mode with the synchronous multiplier phase delay.